Hindawi
Complexity
Volume 2022, Article ID 6035593, 11 pages
https://doi.org/10.1155/2022/6035593

Research Article

Experimental Research on Aerated Supercavitation Suppression of Capillary Outlet Throttling Noise

Qianxu Wang,[1] Shouchuan Wang,[1] Huan Zhang,[1] Yuxuan Wang,[1] Junhai Zhou,[1] Panpan Zhao,[1] and Jia-Bao Liu[2]

[1]*Hefei General Machinery Research Institute Co. Let., Hefei 230000, China*
[2]*School of Mathematics and Physics, Anhui Jianzhu University, Hefei 230601, China*

Correspondence should be addressed to Shouchuan Wang; wangsc0731@163.com

Received 4 September 2021; Revised 4 November 2021; Accepted 6 November 2021; Published 19 January 2022

Academic Editor: Jesus M. Munoz-Pacheco

The aim of this work is the reduction of the throttling noise when the capillary is used as a throttling device. Based on the theory of bubble dynamics, two-phase flow, and aerated supercavitation, four different sizes of aerated devices used in refrigerator refrigeration systems are designed. Throttling noise and the temperature and pressure of inlet and outlet of the capillary are measured under stable operation. To compare the noise suppression effects in different groups of experiments, we introduced the cavitation number to analyze, revealed the principle of aerated supercavitation to suppress noise, and combined the results of Fluent simulations to get the relationship between the noise suppression effect and the aerated quality. The experimental results showed that the aerated device can obviously suppress the throttling noise of the capillary outlet, up to 2.63 dB(A), which provides a new way for reducing the capillary throttling noise.

1. Introduction

In household appliances such as refrigerators that use capillary throttling, noise caused by refrigerant flow is a common problem. Although the refrigerant flow rate is low, it still produces noise that affects the user's life and work in a quiet room, and it also brings hidden dangers to food safety as described by [1]. With the improvement of energy efficiency of household appliances approaching the limit, reducing the noise caused by refrigerant flow to improve acoustic comfort has gradually become a new research hotspot. However, the current research mainly focuses on the fundamental generation mechanism of capillary noise [2–4], there is less research on the technical measures to reduce noise.

Refrigeration equipment operates in a cyclic mode, and the capillary outlet throttling noise determines the overall noise level, especially the cavitation noise, as described by [5, 6], but it has not yet attracted attention [7]. Cavitation noise arises from the transition element between the capillary tube and the evaporator. Reference [3] observed that the connection of this transition structure is usually discontinuous, thus creating conditions for the generation of cavitation noise.

Reference [8] found that the cavitation noise of bubbles is closely related to the pressure pulsation. With the deepening of the research on cavitation noise, it was observed that the size of the cavitation noise is determined by the acoustic characteristics of the bubbles in the tube, as described by [9] and [10]. During the study, they found that the flow pattern is affected by the characteristics of the bubble and established a flow pattern diagram to predict the noise. Reference [11] also studied the fundamental mechanism of capillary outlet noise but did not propose approaches to reduce the noise emission.

Compared with studying the mechanism of cavitation noise, how to reduce the noise is more important. Although [12, 13] achieved the purpose of noise reduction by transforming the transition structure, they did not solve the cavitation noise emission from the root of the noise generation. Reference [14] also tried to use structures such as honeycomb cylinders to adjust flow to reduce noise, but it has certain limitations.

Cavitation was also applied to treat aqueous effluents polluted by organic, toxic, and biorefractory contaminants (2020) [15]. Hydrodynamic cavitation was used for the gradual disintegration of activated sludge and the solubilization of the dissolved organic matter (2021) [16]. Giuseppe Mancuso introduced a hydrodynamic cavitation reactor (Ecowirl) based on swirling jet-induced cavitation and found that Ecowirl reactor resulted in being more energy efficient as compared to hole orifice plates, Venturi and other swirling jet-induced cavitation devices.

In this paper, a noise reduction device is designed based on the theory of bubble dynamics, two-phase flow, and aerated supercavitation, and then the influence of aerated quality change on the noise reduction performance is studied. The fundamental mechanism of noise generation and suppression was analyzed, the noise emission was suppressed from the root of noise generation, and effective noise suppression ideas were innovatively proposed.

2. Theoretical Background for the Root Cause of at the Capillary Outlet

In this section, the theories of two-phase flow and bubble dynamics are reviewed for explaining the root causes of the refrigerant-induced noise that arises at the capillary outlet.

2.1. Two-phase Flow Theory. At any position in the area near the outlet of the capillary, it may be liquid phase, gas phase, or an interface between two phases at different moments. Although the fluid will have inhomogeneities, discontinuities, and uncertainties at any position in the space or in a certain time domain, in principle, the basic equations of fluid mechanics can still be used to establish and analyze the calculation relationship of two-phase flow. Using the split-phase flow model (Figure 1), it is assumed that the gas phase and the liquid phase flow completely separately and have different flow rates. Assuming that the flow is a one-dimensional flow, the pressure distribution of the flow section is uniform, and the change of flow velocity and fluid parameters with the radial direction of the pipeline is ignored, the controlled volume studied is shown in Figure 2, and the angle between the flow and the horizontal direction is θ. The governing equations of the separated-flow model for unidirectional flow are given in (1)–(4), which are the continuity equation, momentum equation, and energy equation, respectively.

Continuity equation is as follows:

$$\frac{\partial(\rho_0 A)}{\partial t} + \frac{\partial(\mathrm{GA})}{\partial z} = 0, \tag{1}$$

where

$$\rho_0 = \left[x v_g + (1-x) v_l\right]^{-1}, \tag{2}$$

where x is the dryness, v_g and v_l are the specific volume of the gas and liquid phases, respectively, G is the mass flux, and A is the cross-sectional area of the pipeline.

Momentum equation is as follows:

$$-\frac{\partial p}{\partial z} = \frac{\tau_w l_w}{A} + \frac{1}{A}\frac{\partial}{\partial z}\left\{\mathrm{AG}^2\left[\frac{x^2 v_g}{\alpha} + \frac{(1-x)^2 v_l}{1-\alpha}\right]\right\} + g\left[\alpha\rho_g + (1-x)\rho_l\right]\sin\theta + \frac{\partial G}{\partial t}, \tag{3}$$

where p is the pressure, τ_w is the shear stress, P_w is the wet perimeter of the control body, α is the cavitation fraction, ρ_g and ρ_l are the density of the gas and liquid phases, and z is the axial coordinates, respectively.

Energy equation is as follows:

$$-\frac{\mathrm{d}p}{\mathrm{d}z} = \rho_0\frac{\mathrm{d}E}{\mathrm{d}z} + \frac{\rho_0}{2}\frac{d}{\mathrm{d}z}\left\{G^2\left[\frac{x^3 v_g^2}{\alpha^2} + \frac{(1-x)^3 v_l^2}{(1-\alpha)^2}\right]\right\} + \rho_0 g\,\sin\theta, \tag{4}$$

where E is the internal energy and ρ_0 is the density after gas-liquid is mixed.

When the flow pattern in a pipe is intermittent (slug, churn (forth), and plug flows), at a specific location in the pipeline, x and α irregularly changing with time, the time gradient of pressure drop is a function of dryness and cavitation fraction as shown in (5) [10]:

$$\frac{d}{\mathrm{d}t}\left(\frac{\mathrm{d}p}{\mathrm{d}z}\right) = \frac{d}{\mathrm{d}t}\left[f(x(t), \alpha(t), \ldots)\right]. \tag{5}$$

This indicates that the pressure of the intermittent flow will fluctuate irregularly, and the pressure fluctuation will act on the pipe wall and then produce obvious vibration and noise. When the flow pattern is annular or bubbly flow, the dryness and cavitation fraction hardly change with time, so the time gradient of pressure drop is very small, and thus the resulting noise sound pressure level is small and basically constant, which is significantly lower than the vibration and noise level of slug flow [5].

2.2. Bubble Dynamics Theory. Bubble dynamics is the theoretical basis for the study of all liquid cavitation phenomena, which has irrelated with cavitation generation methods, cavitation objects, and cavitation shapes. When the molecules in the refrigerant liquid produce thermal movement, temporary microscopic voids will be formed, or they will fracture at the boundary between the solid container wall and the liquid or the boundary between suspended fine particles and the liquid. These weak voids and points constitute the cavitation nucleus necessary for the burst and growth of macroscopic bubble. With the refrigerant flows in the capillary tube, the liquid pressure gradually decreases because of the friction effect in tube, and the saturated liquid refrigerant quickly transforms into a gas-liquid two-phase fluid accompanied by the bubble nucleation process. As the

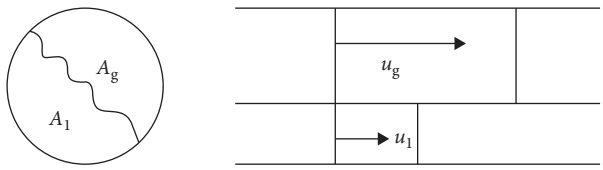

Figure 1: Two-phase and separated-flow model.

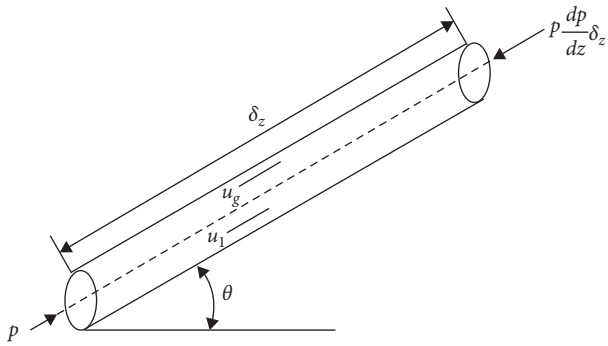

Figure 2: The control volume of the momentum equation of the two-phase and separated-flow model.

superheat of the liquid increases, the nucleation of the inner wall of the pipe and the inside of the liquid will increase significantly. When the static pressure inside the liquid is reduced to a level sufficient to tear the liquid, the cavitation nucleus will inflate, which is called the incipient cavitation [11]. According to the mechanical equilibrium conditions, the pressure in the core can be expressed as

$$P_{g0} = P_0 - P_V + \frac{2S}{R_0}, \tag{6}$$

where P_V is the saturated vapor pressure of the liquid at the corresponding temperature, R_0 is the initial radius of the cavitation nucleus, and S is the surface tension coefficient of the liquid. Regarding bubble frequency, [17] proposed the relationship between bubble radius and natural frequency as showed in

$$f_n = \frac{1}{2\pi R_0}\sqrt{\frac{3\mathrm{kp}}{\rho_l}}. \tag{7}$$

We can observe that the natural frequency of the bubble is closely related to the bubble size. Large bubbles contribute to low frequency, and small bubbles contribute to high frequency.

With the further growth and expansion of the bubble, the bubble will collapse; this process is very rapid and violent. The energy contained in the bubble is released, resulting in strong pressure fluctuations and noise. This process is called bubble collapse. In the refrigeration system, cavitation collapse mainly occurs at the outlet of the capillary tube, and the cavitation noise generated by it makes an important contribution to the flow noise at the outlet of the capillary tube. In order to better describe the characteristics of cavitation, a dimensionless cavitation number σ is introduced in this article:

$$\sigma = \frac{P_\infty - P_V(T_\infty)}{\rho_l u_\infty^2/2}, \tag{8}$$

where P_∞, T_∞, and u_∞ are the hydrostatic pressure, temperature, and velocity on the reference section of the flow field that are not disturbed and ρ_l and P_V are the density of the cavitation liquid medium and the saturated vapor pressure at the corresponding temperature, respectively.

The smaller the cavitation number, the more severe the cavitation degree, but the cavitation intensity is not necessarily high. The cavitation intensity is related to the pressure distribution and flow velocity of the liquid during the flow process and has a direct impact on the cavitation noise. The sound level of the cavitation noise does not rise but falls when it is in the supercavitation state, as described by Arndt [18], which provided a theoretical guidance for reducing capillary flow noise in this paper. The theoretical review shows that the noise induced by refrigerant is closely related to the sound pressure level produced by bubbles. The noise measurement results are mainly introduced in Section 3. The simulation results are combined to analyze the flow field and the noise reduction effect in Section 4. Finally, Section 5 summarizes the paper and outlines future activities.

3. Experimental Methods

3.1. Refrigerator Refrigeration Cycle System. In order to study the flow noise at the outlet of the capillary tube, the paper chooses a refrigerator refrigeration system for experiment. The refrigerator model is Hair BC/BD 103TS. The layout of the refrigeration system is shown in Figure 3. A pressure sensor (PT210B-G1/4) and a temperature sensor (DS18b20) are installed. To measure the inlet and outlet status of the capillary tube, the vortex flow sensor (WL-LWGA-25) is used to measure the mass flow rate. The refrigerant evaporates in the evaporator, takes away the heat, and returns to the compressor. The pressure and temperature of the refrigerant are increased by compression and sent to the condenser. The condensation in the condenser dissipates the heat to the surrounding environment. The refrigerant then flows through the desiccant and the capillary tube and enters the evaporator after throttling, completing the entire cycle. The measurements accuracy is listed in Table 1.

Table 1 lists the experimental measurement data. The data acquisition module is used in conjunction with the software to collect, display, and save the measurement data. The length of the throttling capillary is 3 m, and the inner diameter of the tube is 0.7 mm. The capillary outlet transition tube is shown in Figure 4(a). At the outlet of the capillary, the length of the transition tube is 70 mm, and the capillary extends 20 mm into the transition tube. At the capillary tube outlet, the diameter suddenly expands from 0.7 mm to 6 mm. The optimized transition pipe is equipped with aeration device. As shown in Figure 4(b), four different sizes of aeration devices are designed in this paper, the inner diameters of which are 0.6 mm, 0.8 mm, 1.0 mm, and 1.2 mm, respectively.

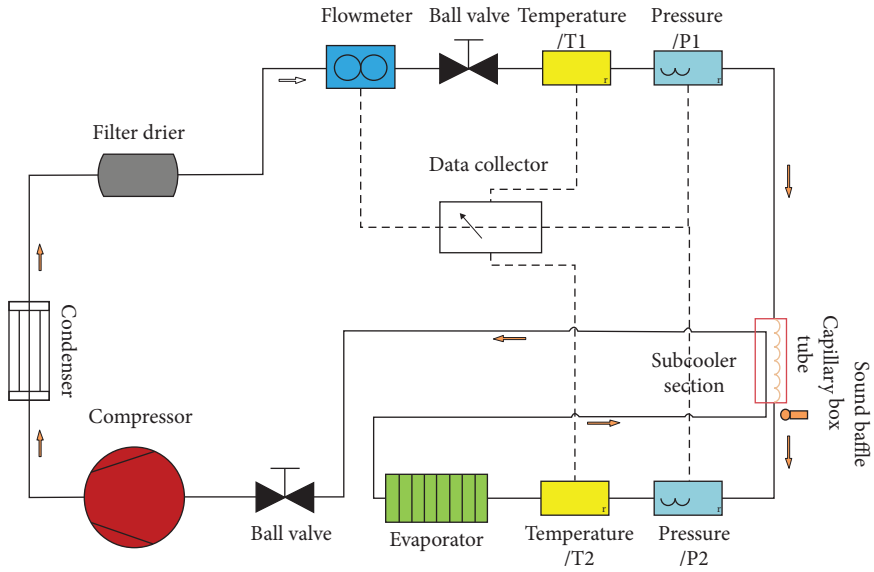

Figure 3: Refrigerator refrigeration system.

Table 1: The calculation parameters of the refrigerator.

Measurand		Value	Uncertainty
Diameter	D_C	0.7 mm	±0.01 mm
	D_S	0.6 mm	±0.01 mm
Length	l_{in}	450 mm	±0.1 mm
	l_{hx}	800 mm	±0.1 mm
	l_c	3050 mm	±0.1 mm
Temperature	T_1	37°C	±0.1°C
	T_2	1°C	±0.1°C
Pressure	P_1	754740 Pa	±100 Pa
	P_2	156960 Pa	±100 Pa
Mass flow	m	0.3 kg h^{-1}	±1%
Capillary roughness		0.00000046	
Refrigerant		R600a	

3.2. Noise Measurement System. The acoustic test system is shown in Figure 5. The portable measurement and analysis system SA-A1 (Japan RION) is used to measure the noise. The 1/2-inch free-field microphone is connected to the host through the preamplifier. The sensitivity of the microphone is −27 (dB re 1 V/Pa)$^{-1}$, the frequency measurement range is 10 Hz to 20000 Hz, and the maximum measurement noise value is 148 dB. The system fully meets the measurement requirements of the experiment. The data measured in the experiment is processed by the SA-A1 system host and supporting software.

There is a sound-proof baffle box in the transition area between the capillary tube and the evaporator, which is covered with sound-absorbing material and also has good heat insulation performance. In order to reduce the presence of moisture that may cause the formation of hoarfrost, the test area was designed to be as small as possible, and the detection area inside the box is $(100 \times 100 \times 100)$ mm^3. In addition, silica gel can dehumidify the enclosed air. The pipe section in the box is not insulated to achieve a better signal-to-noise ratio. The microphone is located 10 mm above the capillary outlet.

For frequencies above 250 Hz, the third-octave band analysis of the background noise measurement corresponds to the inherent noise of the microphone. Below 250 Hz, acoustic disturbances caused by the compressor affect the sound measurements. In order to avoid the necessity of a complex background noise correction, the acoustic analysis is carried out in frequency band of 250 Hz to 16000 Hz. To calculate the A-weighted sound pressure level, the standardized time weighting span "fast" with an exponential average aging time of 125 ms is used.

In a refrigerator, the refrigerant flow cavitation noise frequency is basically the same as the natural frequency of the bubble, and the natural frequency of the bubble can be calculated by (7) as described in [17]. By measuring the noise value under different aeration devices, the correlations between the noise suppression effect and the aeration quality can be obtained.

3.3. Experimental Setup. The refrigerator located on a 5-6 mm thick elastic rubber pad make it run under no load, adjust the thermostat to a medium or strong cold position, and start the

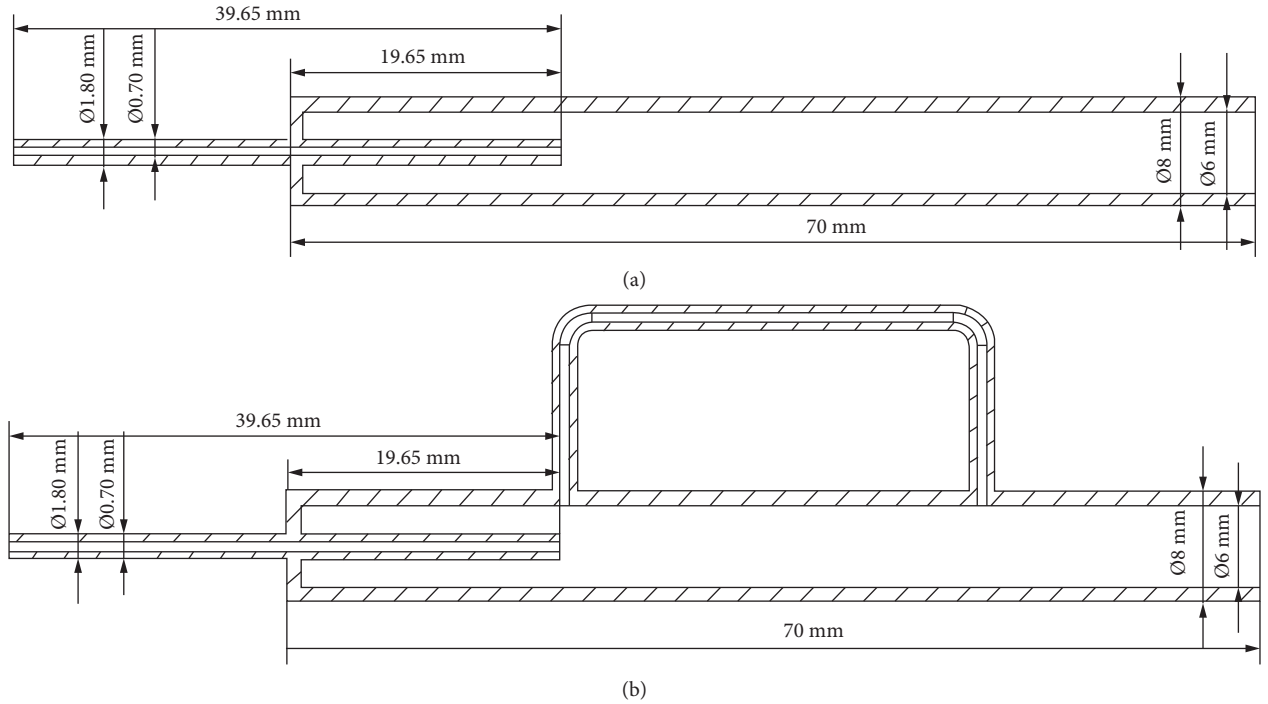

Figure 4: Transition pipe of the refrigeration system. (a) Transition pipe and (b) transition pipe equipped with aeration device.

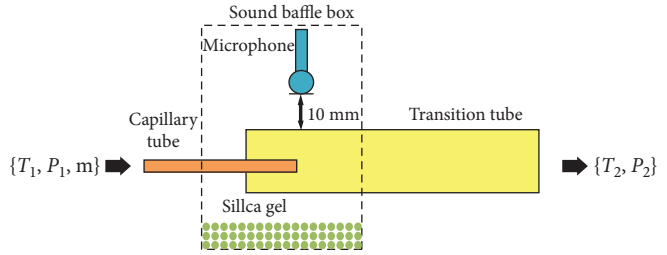

Figure 5: Setup of the sound baffle box around the capillary tube outlet.

test after running for at least 30 minutes. During the test, Because the temperature in the box has reached the set temperature and the machine is stopped, the measurement needs to be interrupted, and the measurement should be performed after the compressor restarts for 3 minutes.

Temperature and pressure sensors are installed at the inlet and outlet of the capillary tube, respectively. Because the refrigerant at the outlet of the condenser is in a supercooled state and single-phase flow, the flowmeter is installed here to measure the refrigerant flow of the refrigeration system. We install aeration devices of different sizes to optimize the transition structure of the refrigerator and repeat the above steps to conduct the experiment. Through the installation of aeration devices, local supercavitation is achieved and the purpose of suppressing refrigerant cavitation is achieved. Four different sizes of aeration devices are used, the inner diameters of which are 0.6 mm, 0.8 mm, 1.0 mm, and 1.2 mm, respectively.

The ambient temperature and humidity are 20.5°C/73%, respectively, and the atmospheric pressure is 1.0118×10^5 Pa. The temperature of the fresh-keeping chamber was set at 6°C.

3.4. Flow Simulation at the Capillary Outlet. Combined with the previous experimental results, the commercial simulation software Fluent was used to simulate the flow at the capillary outlet. As shown in Figure 2, the capillary flow model was established, the mixture multiphase flow model and energy equation was selected, the Schnerr and Sauer cavitation model and the reliable k-e turbulence model were selected, cavitation properties choose tabular-pt-sat, bubble number density of model constants setting is $1e^8$, and turbulent coefficient setting is 0.39. The wall function selected Standard Wall Functions and turbulent viscosity is none. The refrigerant of R600a was selected as the materials in fluid and reference temperature was set to 303 k. The boundary conditions were selected pressure inlet (754740 Pa) and pressure outlet (156960 Pa), total temperature of inlet is set to 303.15 k, and total temperature of outlet is set to 283.15 k. Specification method of turbulence selected k and epsilon, turbulent kinetic energy was set to 0.02 m^2/s^2, and turbulent dissipation rate was set to 1 m^2/s^3. The solution method was set to coupled solution; pseudo transient was selected at the same time. Moment, turbulent

kinetic energy, turbulent dissipation rate, and energy were set to second order upwind; others keep the default settings. Refer to Table 1 for specific parameter settings. Take the capillary inlet and outlet flow rate and its degree of change as the judgment standard to judge whether the entire capillary model calculation process has converged. The calculated residual values are all set to less than 10^{-6}, when the capillary inlet and outlet flow does not change with the time. When the capillary inlet and outlet flow rate changes less than 5%, it can be determined that the capillary model calculation results at this time have converged. The capillary models with 2.79 million grids, 4 million grids, and 6 million grids were calculated, and the three simulation results were compared. The difference between the latter two was less than 0.5%. Finally, 4 million grids were selected to complete the calculation.

4. Results and Analysis

4.1. Noise Reduction of Aerated Supercavitation. A aeration device ($D4 = 0.8$ mm) was selected to verify the noise reduction effect, and the time domain and frequency domain diagrams of the flow noise at the capillary outlet during the stable operation of the refrigerator were obtained, which can be observed from the time domain diagram (Figure 6). When the aeration device was not installed, the overall noise value of the capillary outlet is relatively large, reaching to 26.4 dB(A). After the aeration device was installed, the flow noise of the capillary outlet is significantly lower than the noise of the capillary outlet not equipped with aeration device. The noise fluctuation is more stable, the noise value is only 24.4 dB(A), and the noise suppression value is 2 dB(A). Thus, the aeration device has a significant effect on the flow noise suppression of the capillary outlet.

It can be observed from the frequency distribution (Figure 7) that the maximum noise frequency of the capillary outlet is mainly distributed from 200 Hz to 2000 Hz, indicating that the noise at these frequencies plays a decisive role in the flow noise of the capillary outlet, as also described by [13].

When the refrigeration system is operating stably, the temperature of the capillary outlet was measured with time. From the temperature time domain diagram (Figure 8), it can be observed that the inlet and outlet temperatures of the capillary are 37.5°C/−13.5°C, respectively. After the aeration, the temperature of the capillary inlet and outlet is also 37.5°C/−13.5°C, respectively, indicating that the aeration device has no effect on the temperature of the capillary inlet and outlet, and it does not affect the refrigeration effect of the entire refrigerator refrigeration system.

4.2. The Correlations between Cavitation Noise Frequency and Aeration Quality. The frequency range of refrigerant bubble collapse was calculated to be 200 Hz–2000 Hz; according to (7), the influence of the installation of 4 different aeration devices on the noise frequency of the capillary outlet was measured, and the frequency distribution diagram was obtained as shown in Figure 9. Through analysis, it can be found that the main noise frequency distribution of the capillary outlet under the four working conditions is distributed in 200 Hz–2000 Hz. Combining Figure 7 to analyze, it can be known that the noise at these frequencies is mainly cavitation noise caused by cavitation phenomenon.

By calculating the aeration quality of different aeration devices, the aeration quality of different aeration devices is obtained as shown in Table 2. The size of the aeration device affects the aeration quality, and the aeration quality increases from $1.37 \times 10^{-4}\,\mathrm{kg\,s^{-1}}$ to $5.48 \times 10^{-4}\,\mathrm{kg{\cdot}s^{-1}}$. Despite changing the aeration quality, the maximum noise frequency is still distributed between 200 Hz and 2000 Hz, indicating that the aeration device will not affect the frequency range of cavitation noise.

4.3. The Correlations between Cavitation Noise Suppression Effect and Aeration Quality. The experiment was carried out using the original transition pipe and four transition pipes with different sizes of aeration devices. Moreover, in order to ensure the accuracy of the experiment, the experiment was repeated once. The noise measurement data was analyzed and calculated, and the noise suppression value comparison chart was obtained (Figure 10). Analyzing Figure 10, it can be observed that the experimental results remain unchanged when conducting experiments again. When the aeration quality increases from $1.37 \times 10^{-4}\,\mathrm{kg\,s^{-1}}$ to $5.48 \times 10^{-4}\,\mathrm{kg{\cdot}s^{-1}}$, the value of noise suppression first increases and then decreases. When the diameter of the aeration pipe is $D5 = 1.0$ mm, the aeration quality is $3.84 \times 10^{-4}\,\mathrm{kg{\cdot}s^{-1}}$. Under this condition, the noise suppression value is 2.63 dB(A), which had the best noise suppression effect on the outlet of the refrigerator capillary.

In order to further explain the influence of the aeration quality on the cavitation noise suppression effect, the cavitation number (σ) was introduced to characterize the cavitation phenomenon. Calculate the cavitation number in the local area of the capillary outlet according to (8). The specific value is shown in Table 2. When the cavitation number σ is 0.12 to 0.2, it represented the local cavitation stage. Under this condition, the noise level increases as the cavitation number decreases. and the sound level of cavitation noise did not rise but fell as the cavitation number decreased. When the cavitation number (σ) is below 0.12, it represented the supercavitation status, as confirmed by [18, 19]. From the cavitation number calculated in the paper, it can be clearly observed that the local cavitation number is lower than 0.07 after aeration. Thus, the supercavitation state is locally realized, and the noise level decreases with the decrease of the cavitation number (σ). When $D_5 = 1$ mm, the cavitation number (σ) is 0.057 and the noise level is reduced the most, which is consistent with the results of the previous experimental measurements.

4.4. Simulation Results. Aeration is performed locally on the capillary outlet, and the pressure distribution on the axis of the capillary outlet is shown in Figure 11. The zero point on the x-axis represents the capillary outlet. It can be observed that the aeration device can significantly increase the partial

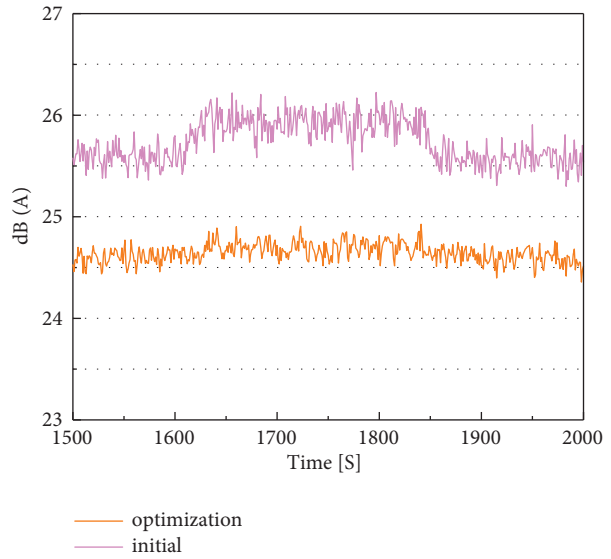

Figure 6: Time domain diagram of the noise of the capillary outlet before and after aeration.

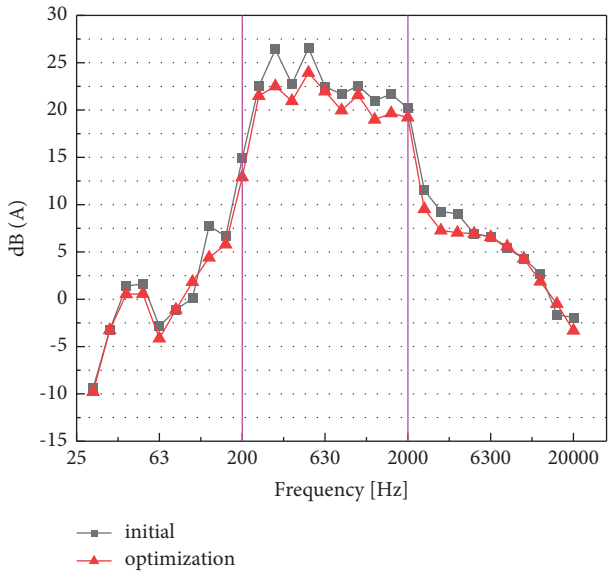

Figure 7: Frequency domain diagram of the noise of capillary outlet before and after aeration.

pressure of the capillary outlet, and it can also be found that $D6 = 1.2$ mm aeration device contributes the most to the local pressure increase, increasing by 800 Pa from Figure 11, indicating that the partial pressure of the capillary outlet is significantly affected by the quality of aeration.

Analyzing the refrigerant gas volume distribution diagram on the outlet axis of the capillary tube (Figure 12), at a position 0 m away from the capillary outlet, the local gas content between the initial transition tube and the four transition tubes with different aeration devices was compared. It is found that the gas content of the local refrigerant at the outlet of the capillary was significantly increased after aeration. When the diameter of the aeration devices is $D6 = 1.2$ mm and the aeration quality is 5.48×10^{-4} kg·s^{-1}, the vapor rate increase is 0.1 under this condition, indicating that the greater is the quality of aeration, the more beneficial it is to increase the local refrigerant vapor rate.

In order to better explain the vapor rate distribution diagram (Figure 12), Figure 12 was divided into four areas I, II, III, and IV. It can be observed that when the aeration device is not installed, the refrigerant bubble gradually grows and matures in the area of II, the gas volume fraction gradually increases from 0.79 to 0.86, then the refrigerant bubble begins to collapse in the III area, the gas volume fraction gradually decreases to 0.80, and finally the collapse is complete in the IV area. The volume fraction gradually stabilized to 0.79. When the aeration amount is 2.43×10^{-4} kg·s^{-1}, the partial pressure of the capillary outlet is increased, but the process of bubble

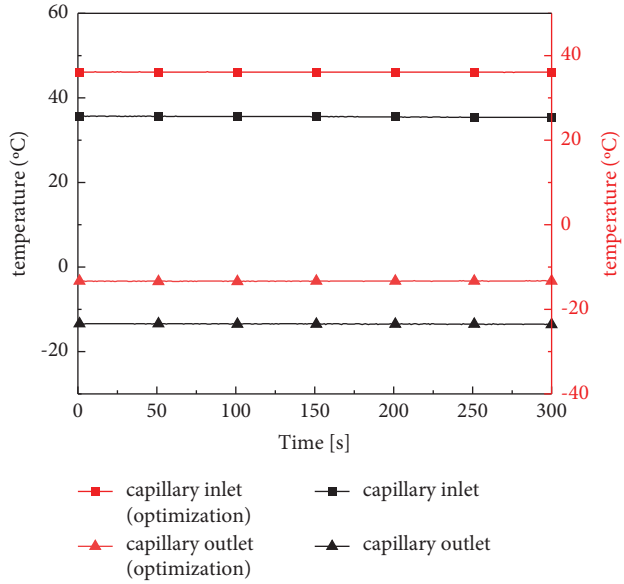

Figure 8: The temperature of the capillary inlet and outlet before and after aeration.

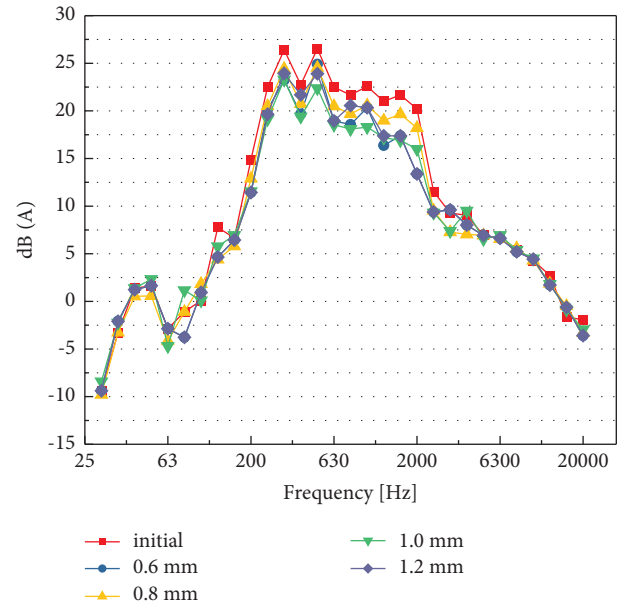

Figure 9: Frequency domain diagram of noise distribution equipped with different sizes of aeration devices.

Table 2: Aeration quality and cavitation number.

Aeration device pipe diameter D (mm)	Aerated amount q (kg·s^{-1})	Cavitation number σ
0.6	1.37×10^{-4}	0.068
0.8	2.43×10^{-4}	0.062
1.0	3.84×10^{-4}	0.057
1.2	5.48×10^{-4}	0.061

growth, maturation, and collapse still occurs, and the gas volume fraction still changes significantly, but when the aeration amount is greater than 2.43×10^{-4} kg·s^{-1} at this time, the bubble growth and collapse process was significantly suppressed, and the gas phase volume fraction remained basically steadily, indicating that the cavitation

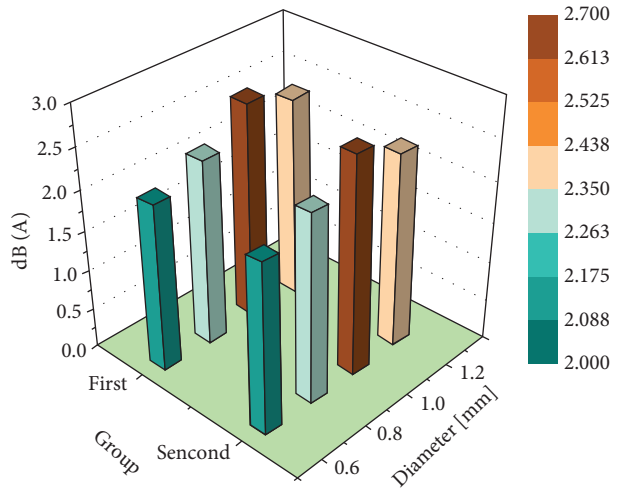

Figure 10: The value of noise suppression aerated different quality refrigerant.

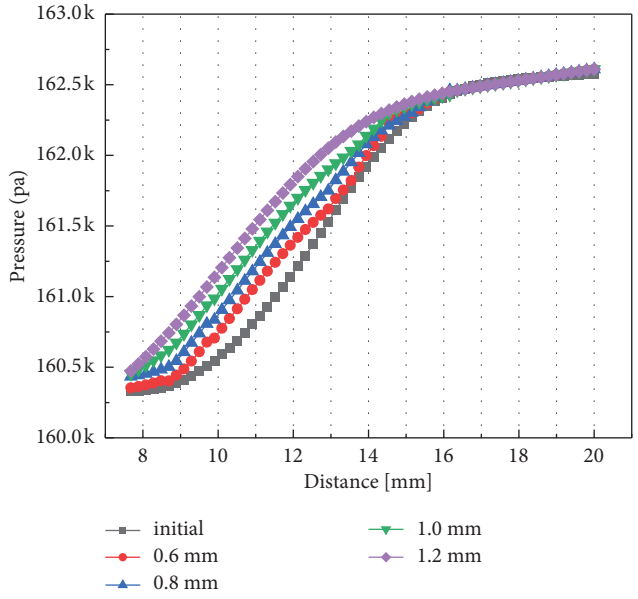

Figure 11: Local pressure distribution at the capillary outlet.

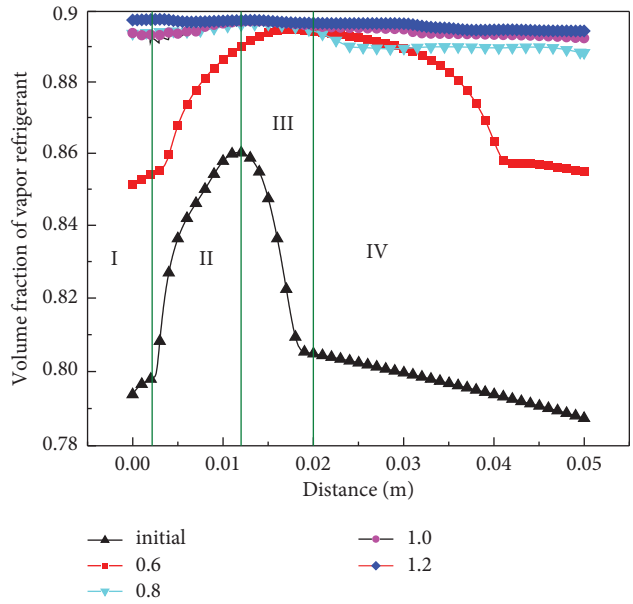

Figure 12: Local refrigerant vapor rate distribution at the outlet of the capillary.

phenomenon was suppressed. Therefore, conclusion can be made that the aeration devices can effectively reduce the cavitation noise.

5. Conclusion

Acoustic investigations are carried out at the outlet of a capillary tube, which serves as a throttling device in a vapor compression cycle. The refrigerator refrigeration system was used to study the flow noise of the capillary outlet, analyze the characteristics of the noise frequency distribution at the capillary outlet, and find that the main noise frequency distribution range of 200 Hz to 2000 Hz at the capillary outlet.

Under the same experimental conditions, aeration devices of different sizes were selected for experiments. By introducing a dimensionless parameter cavitation number σ, the principle of aeration supercavitation noise suppression was explained, and the correlations between noise frequency distribution, noise suppression effect, and aeration quality were found.

Finally, fluent software was used to simulate the flow at the capillary outlet to further verify the experimental results. Through experimental study and analysis, it is determined that cavitation noise is the main contributor to the capillary outlet throttling noise, and the feasibility of noise reduction of the aeration device is verified. At the same time, the suppression effect of different sizes of aeration devices on the noise value was obtained; it can reach up to 2.63 dB(A). Moreover, the aeration device has no negative influence on the evaporation temperature and normal operation of the refrigerator. The aeration device can significantly increase the local pressure, form supercavitation, and suppress the cavitation noise.

The previous article only proves that the aeration device can reduce the flow noise at the capillary outlet (2021). Based on the previous article, this article further studies the influence of different aeration quality on the noise suppression effect. The relationship between aeration quality and noise suppression lays a theoretical foundation for the application of aeration devices.

The noise generation process is very complicated and cannot be determined according to the given initial conditions. When the supercavitation state is reached, the cavitation noise decreases with the decrease of the cavitation number. In this paper, the internal diameter $D = 1.0$ aeration device is selected to achieve the best noise suppression effect. However, for different initial conditions, the influence of the aeration device size change on the cavitation number is different; this is the study of chaos.

The research in this article also provided reference value for noise suppression of other throttling devices.

Abbreviations

E: Internal energy (kJ)
D: Inner diameter (mm)
L: Length (mm)
T: Temperature (°C)
P: Pressure (Pa)
R: Radius (mm)
S: Liquid surface tension coefficient
M: Mass flow (kg s^{-1})
X: Dryness
U: Velocity (m s^{-1})
v: Specific volume
G: Mass flux (kg s^{-1})
A: Pipe cross-sectional area (m^2)
P: Density (kg m^{-3})
Z: Axial coordinates (m)
Q: Aeration amount (kg s^{-1})

Greek symbols
Σ: Cavitation number
A: Vacuole share
T: Shear stress
Λ: Capillary roughness

Subscripts
C: Capillary
S: Compressor suction pipe
W: Control body
O: Gas-liquid two-phase
V: Liquid saturated steam
∞: Reference section
in: Capillary before exchanging heat with compressor suction pipe
hx: Capillary exchanging heat with compressor suction pipe
1: Capillary inlet
2: Capillary outlet
3: 0.8 mm diameter aeration device
4: 1.0 mm diameter aeration device
5: 1.2 mm diameter aeration device
6: 1.4 mm diameter aeration device.

Data Availability

The figure and table data used to support the findings of this study are available from the corresponding author upon request.

Conflicts of Interest

The authors declare that they have no known competing financial interesting or personal relationships that could have appeared to influence the work reported in this paper.

References

[1] W. Hofstetter Richard, E. Copp Brennan, and I. Lukic, "Acoustic noise of refrigerators promote increased growth rate of the gray mold Botrytis cinereal," *Journal of Food Safety*, vol. 40, no. 6, 2020.

[2] D. Hartmann and C. Melo, "An experimental study on the capillary tube flow and its effect on the acoustic behavior of household refrigeators," in *Proceedings of the 15th International Refrigeration and Air Conditioning Conference*, pp. 1367–1378, IRAC, West Lafayette, Indiana, 14 July 2014.

[3] T. Tannert and U. Hesse, "Noise effects in capillary tubes caused by refrigerant flow," in *Proceedings of the 16th International Refrigeration and Air Conditioning Conference*, pp. 1562–1572, IRAC, West Lafayette, Indiana, 11 July 2016.

[4] Y.-Z. Wu, Z. Rui-Qi, X.-L. Cao, and G. Yan, "Combined nucleation theory and models for refrigerant flow in a capillary tube," *Journal of Xi'an Jiaotong University*, vol. 36, no. 7, pp. 661–664, 2002.

[5] H. S. Han, W. B. Jeong, M. S. Kim, and T. H. Kim, "Analysis of the root causes of refrigerant-induced noise in refrigerators," *Journal of Mechanical Science and Technology*, vol. 23, no. 12, pp. 3245–3256, 2009.

[6] H. S. Han, W. B. Jeong, M. S. Kim, S. Y. Lee, and M. Y. Seo, "Reduction of the refrigerant-induced noise from the evaporator-inlet pipe in a refrigerator," *International Journal of Refrigeration*, vol. 33, no. 7, pp. 1478–1488, 2010.

[7] Q. Wang, Y. Liu, Y. Yao, and Yu Zhang, "Experimental study of vapor supercavitation suppression of capillary outlet jet noise[J]," *Journal of Mathematics*, vol. 2021, Article ID 9936291, 10 pages, 2021.

[8] K. Tatsumi, "Study on noise caused by slug flow through a capillary tube (in Japanese)[J]," *Transactions of the Japan Society of Mechanical Engineers: Serie Bibliographique*, vol. 64, no. 611, pp. 2392–2397, 1997.

[9] H. S. Han, W. B. Jeong, and M. S. Kim, "Frequency characteristics of the noise of R600a refrigerant flowing in a pipe with intermittent flow pattern," *International Journal of Refrigeration*, vol. 34, no. 6, pp. 1497–1506, 2011.

[10] M. S. Kim, W. B. Jeong, and H. S. Han, "Development of noise pattern map for predicting refrigerant-induced noise in refrigerators," *Journal of Mechanical Science and Technology*, vol. 28, no. 9, pp. 3499–3510, 2014.

[11] J. Ruebeling and S. Grohmann, "Flow-induced noise generation at the outlet of a capillary tube[J]," *International Journal of Refrigeration*, vol. 111, 2020.

[12] B. Demirtekin and A. S. Sarigül, "Flow-induced noise in refrigerators (conference paper)," in *Proceedings of the International Noise Conference*, Institute of Noise Control Engineering, Hamburg, Germany, August 2016.

[13] X. I. A. Yu-bo, L. I. U. Yong-hui, L. I. U. Yi-cai, Y. Ma, C. Xiao, and T. Wu, "Experimental study on reducing the noise of horizontal household freezers," *Applied Thermal Engineering*, vol. 68, no. 1/2, pp. 107–114, 2014.

[14] G. Kim and S. Song, "Noise reduction of refrigerant two-phase flow using flow conditioners near the electric expansion valve," *Journal of Mechanical Science and Technology*, vol. 34, no. 2, pp. 719–725, 2020.

[15] C. Earls Brennen, *Cavitation and Bubble dynamics*, Jiangsu University Press, Zhenjiang, China, 2013.

[16] J. Cai, *Application of Liquid Cavitation technology[M]*, Science Press, Beijing, China, 2019.

[17] M. Minnaert, "XVI.On musical air-bubbles and the sounds of running water," *The London, Edinburgh, and Dublin Philosophical Magazine and Journal of Science*, vol. 16, no. 104, pp. 235–248, 1933.

[18] R. E. A. Arndt, "Recent advances in cavitation research," *Advances in Hydroscience*, vol. 12, pp. 1–78, 1981.

[19] Y. A. N. Chang-qi, *Gas-liquid Two-phase flow[M]*, pp. 38–64, Harbin Engineering University Press, Harbin, China, 2017.